JOURNAL OF GEOPHYSICAL RESEARCH, VOL. 113, A06301, doi:10.1029/2007JA012911, 2008

Radiation of ELF/VLF waves by harmonically varying currents into a stratified ionosphere with application to radiation by a modulated electrojet

N. G. Lehtinen[1] and U. S. Inan[1]

Received 26 October 2007; revised 3 January 2008; accepted 26 February 2008; published 3 June 2008.

[1] We use a full-wave finite element approach inspired by the mode calculation method of Wait (1970) to calculate electromagnetic fields in a horizontally stratified ionosphere treated as a magnetized plasma. The source currents can have arbitrary vertical and horizontal distributions. The electromagnetic field is calculated both in the Earth-ionosphere waveguide (at arbitrary horizontal distance and direction) and in the ionosphere (as an upward propagating whistler mode wave). This method requires less computational resources than traditional FDFD and FDTD methods, while providing results with similar accuracy. The model is applied to the radiation of ELF/VLF waves from modulated HF-heated electrojet currents, and the calculated values are compared to ground and satellite observations.

Citation: Lehtinen, N. G., and U. S. Inan (2008), Radiation of ELF/VLF waves by harmonically varying currents into a stratified ionosphere with application to radiation by a modulated electrojet, *J. Geophys. Res.*, *113*, A06301, doi:10.1029/2007JA012911.

1. Introduction

[2] There is a plethora of methods for finding fields in stratified media [*Wait*, 1970; *Bossy*, 1979; *Yagitani et al.*, 1994; *Nygrén*, 1981; *Nagano et al.*, 1994], which are summarized, e.g., by *Budden* [1985, chapter 18]. However, many of them have difficulty with numerical stability when the evanescent wave solutions (with a large imaginary component of the vertical wave number) "swamp" the waves of interest, which requires special tricks to contain the stability [*Pitteway*, 1965; *Nygrén*, 1982]. A detailed discussion of this effect can be found in the work of *Budden* [1985, pp. 574–576]. Here we describe a method which is inherently stable against such "swamping." It is based on the idea of recursive calculation of reflection coefficients and mode amplitudes by *Nygrén* [1982] and also allows the use of an arbitrary configuration of the radiating sources.

2. Description of the Method

2.1. Waves in Stratified Medium

[3] Consider electromagnetic waves with time dependence $\sim e^{-i\omega t}$ in a horizontally stratified ionosphere. Let us choose a coordinate system with a vertical upward z-axis (perpendicular to the layers) and x, y axes in the horizontal plane. We divide the medium into layers with boundaries z_k, $k = 1 \ldots M$ [*Wait*, 1970], with $z_1 = 0$ corresponding to the ground. In each layer $\Omega_k = (z_k, z_{k+1})$ (where $k = 1 \ldots M - 1$) and $\Omega_M = (z_M, \infty)$, the medium is assumed to be uniform, with permeability $\mu = 1$ and permittivity (at given frequency ω) described by the tensor $\hat{\varepsilon}_k$. The thickness of layer Ω_k is $h_k = z_{k+1} - z_k$, $k = 1 \ldots M - 1$.

[4] Maxwell's equations for a source-free medium are (in layer Ω_k)

$$\nabla \times \mathbf{H} = -ik_0 \hat{\varepsilon}_k \mathbf{E} \tag{1}$$

$$\nabla \times \mathbf{E} = ik_0 \mathbf{H} \tag{2}$$

where $k_0 = \omega/c$ and for convenience we use SI units for $\mathbf{E}$ and modified units for $\mathbf{H}$, so that $\mathbf{H} = Z_0 \mathbf{H}_{\mathrm{SI}}$ [*Budden*, 1985, p. 31], where $Z_0 = \sqrt{\mu_0/\varepsilon_0}$ is the impedance of free space.

[5] We seek a solution in a form of a linear combination of plane waves $\sim e^{ik_0(\mathbf{n}\cdot\mathbf{r})}$ in each layer, where $\mathbf{n}$ is the refractive index vector, whose horizontal component $\mathbf{n}_\perp$ is conserved by Snell's law, so that n_x = const, n_y = const. Inside each layer, we have

$$\mathbf{n} \times \mathbf{H} = -\hat{\varepsilon}\mathbf{E} \tag{3}$$

$$\mathbf{n} \times \mathbf{E} = \mathbf{H} \tag{4}$$

Substituting the second equation into the first, we find an equation for $\mathbf{E}$

$$\left(n^2 \mathsf{I} - \mathbf{n}\mathbf{n}^T - \hat{\varepsilon}\right)\mathbf{E} = 0 \tag{5}$$

and the dispersion equation

$$\det\left(n^2 \mathsf{I} - \mathbf{n}\mathbf{n}^T - \hat{\varepsilon}\right) = 0 \tag{6}$$

where I is a unit tensor and $\mathbf{n}\mathbf{n}^T$ is a diadic product.

[1]STARLab, Electrical Engineering Department, Stanford University, Stanford, California, USA.

0148-0227/08/2007JA012911$09.00

[6] The dispersion equation (6), when written as an equation for n_z, is a quartic equation which is usually called the Booker quartic [*Booker*, 1938]. We use a standard method to solve it [e.g., *Abramowitz and Stegun*, 1970, p. 17]. In general, this equation has four roots $n_z^{(m)}$, $m = 1 \ldots 4$, with a possibility of multiple roots. We sort the four solutions obtained for n_z according to their imaginary part. A positive imaginary part means that the wave is evanescent or absorbed in the upward direction, and negative means that the wave is evanescent or absorbed in the downward direction. On the basis of this reasoning, we label the two modes corresponding to the higher imaginary parts of n_z as upward propagating and the other two modes as downward propagating and denote $n_z^{u1} \equiv n_z^{(1)}$, $n_z^{u2} \equiv n_z^{(2)}$, $n_z^{d1} \equiv -n_z^{(3)}$, $n_z^{d2} \equiv -n_z^{(4)}$, so that all n_z^{ui}, n_z^{di}, $i = 1, 2$, have nonnegative imaginary parts.

[7] The field structure of each mode (components of $\mathbf{E}^{(m)}$, $\mathbf{H}^{(m)}$) is found from (5) and (4), with arbitrary normalization. We can choose, e.g., $|\mathbf{E}^{(m)}|^2 = 1$. These components make up a 6×4 matrix, which is constant in each layer Ω_k. We denote this matrix $\mathcal{F}_k$, with components $(\mathcal{F}_k)_{1,m} = E_x^{(m)}$, $(\mathcal{F}_k)_{2,m} = E_y^{(m)}$ etc. The fields are obtained using these matrices from the upward and downward propagating mode amplitudes $\mathbf{u}(z)$ and $\mathbf{d}(z)$, respectively:

$$\begin{pmatrix} \mathbf{E}(\mathbf{r}) \\ \mathbf{H}(\mathbf{r}) \end{pmatrix} = \mathcal{F}_k \begin{pmatrix} \mathbf{u}(z) \\ \mathbf{d}(z) \end{pmatrix} e^{ik_0(\mathbf{n}_\perp \cdot \mathbf{r}_\perp)} \quad \text{in layer } \Omega_k \tag{7}$$

where $\mathbf{u}$ and $\mathbf{d}$ are arrays of length 2:

$$\mathbf{u} = \begin{pmatrix} u^1 \\ u^2 \end{pmatrix}, \quad \mathbf{d} = \begin{pmatrix} d^1 \\ d^2 \end{pmatrix} \tag{8}$$

For example, in an isotropic medium ($\hat{\varepsilon} \equiv \varepsilon$, $n_\perp^2 + n_z^2 = n^2 = \varepsilon$) we can choose the TE mode for u^1 and d^1 and the TM mode for u^2 and d^2:

$$\mathcal{F}_{\text{isotropic}} = \begin{pmatrix} -\sin\phi & (n_z/n)\cos\phi & -\sin\phi & (n_z/n)\cos\phi \\ \cos\phi & (n_z/n)\sin\phi & \cos\phi & (n_z/n)\sin\phi \\ 0 & -n_\perp/n & 0 & n_\perp/n \\ -n_z\cos\phi & -n\sin\phi & n_z\cos\phi & n\sin\phi \\ -n_z\sin\phi & n\cos\phi & n_z\sin\phi & -n\cos\phi \\ n_\perp & 0 & n_\perp & 0 \end{pmatrix} \tag{9}$$

where $\cos\phi = n_x/n_\perp$, $\sin\phi = n_y/n_\perp$.

[8] We are interested mostly in the horizontal components of $\mathbf{E}$, $\mathbf{H}$, since they have to be continuous at the boundaries between layers in the absence of sources. These components are given by a 4×4 matrix F_k which is a submatrix of $\mathcal{F}_k$:

$$\begin{pmatrix} \mathbf{E}_\perp(z) \\ \mathbf{H}_\perp(z) \end{pmatrix} = \mathsf{F}_k \begin{pmatrix} \mathbf{u}(z) \\ \mathbf{d}(z) \end{pmatrix} \quad \text{in layer } \Omega_k \tag{10}$$

(we do not include the factor $e^{ik_0(\mathbf{n}_\perp \cdot \mathbf{r}_\perp)}$ in $\mathbf{E}_\perp$, $\mathbf{H}_\perp$). In each layer Ω_k, $\mathbf{u}(z)$ and $\mathbf{d}(z)$ are given in terms of their values at $z_k + 0$ (i.e., just above the boundary z_k), which we denote as $\mathbf{u}_k$ and $\mathbf{d}_k$:

$$u^i(z) = u_k^i e^{ik_0 n_z^{ui}(z - z_k)} \tag{11}$$

$$d^i(z) = d_k^i e^{-ik_0 n_z^{di}(z - z_k)}, \quad i = 1, 2 \tag{12}$$

At $z = z_{k+1} - 0$ (still in the layer Ω_k, just below the boundary z_{k+1}), we have

$$\mathbf{u}'_{k+1} \equiv \mathbf{u}(z_{k+1}) = \mathsf{P}_k^{\text{u}} \mathbf{u}_k \tag{13}$$

$$\mathbf{d}'_{k+1} \equiv \mathbf{d}(z_{k+1}) = \left(\mathsf{P}_k^{\text{d}}\right)^{-1} \mathbf{d}_k \tag{14}$$

where P^{u}, P^{d} describe propagation in a uniform medium over layer Ω_k:

$$\mathsf{P}^{\text{u}} = \begin{pmatrix} e^{ik_0 n_z^{u1} h_k} & 0 \\ 0 & e^{ik_0 n_z^{u2} h_k} \end{pmatrix} \tag{15}$$

$$\mathsf{P}^{\text{d}} = \begin{pmatrix} e^{ik_0 n_z^{d1} h_k} & 0 \\ 0 & e^{ik_0 n_z^{d2} h_k} \end{pmatrix} \tag{16}$$

Owing to the way we chose n_z^{ui}, n_z^{di} to have nonnegative imaginary parts, the matrices P^{u}, P^{d} have bounded norms (the amplitude of the wave is nonincreasing as it propagates), a fact which allows us to devise a stable method of finding the fields.

[9] The fields $\mathbf{E}_\perp$, $\mathbf{H}_\perp$ are continuous at each boundary z_k, $k = 2 \ldots M$ (in the absence of sources). Therefore, we have a boundary condition

$$\mathsf{F}_k \begin{pmatrix} \mathbf{u}'_{k+1} \\ \mathbf{d}'_{k+1} \end{pmatrix} = \mathsf{F}_{k+1} \begin{pmatrix} \mathbf{u}_{k+1} \\ \mathbf{d}_{k+1} \end{pmatrix} \tag{17}$$

From these equations, we can find matrices for transport through boundary z_{k+1}:

$$\begin{pmatrix} \mathbf{u}'_{k+1} \\ \mathbf{d}'_{k+1} \end{pmatrix} = \mathsf{T}^{\text{d}}{}_k \begin{pmatrix} \mathbf{u}_{k+1} \\ \mathbf{d}_{k+1} \end{pmatrix} \tag{18}$$

$$\begin{pmatrix} \mathbf{u}_{k+1} \\ \mathbf{d}_{k+1} \end{pmatrix} = \mathsf{T}^{\text{u}}{}_k \begin{pmatrix} \mathbf{u}'_{k+1} \\ \mathbf{d}'_{k+1} \end{pmatrix} \tag{19}$$

where T_k^{u} and T_k^{d} are inverses of each other and are given by

$$\mathsf{T}_k^{\text{d}} = \mathsf{F}_k^{-1} \mathsf{F}_{k+1} \tag{20}$$

$$\mathsf{T}_k^{\text{u}} = \mathsf{F}_{k+1}^{-1} \mathsf{F}_k \tag{21}$$

If the medium does not change at the boundary z_{k+1}, then T_k^{u} and T_k^{d} should be unit matrices.

2.2. Reflection Coefficients

[10] Introduce R_k^{u} and R_k^{d} as the reflection coefficients for waves travelling up and down, respectively, so that

$$\mathbf{d}_k = \mathsf{R}_k^{\text{u}} \mathbf{u}_k \tag{22}$$

if all sources are located below z_k, and

$$\mathbf{u}_k = \mathsf{R}_k^{\text{d}} \mathbf{d}_k \tag{23}$$

if all sources are located above z_k. We now demonstrate that there is no "swamping" instability if $\mathsf{R}^{\mathrm{u}}_k$ is calculated entirely in terms of $\mathsf{R}^{\mathrm{u}}_{k+1}$, and $\mathsf{R}^{\mathrm{d}}_{k+1}$ is calculated entirely in terms of $\mathsf{R}^{\mathrm{d}}_k$.

[11] Let us consider a wave propagating upward which reflects at boundary z_{k+1} with a known reflection coefficient $\mathsf{R}^{\mathrm{u}}_{k+1}$, so that $\mathbf{d}_{k+1} = \mathsf{R}^{\mathrm{u}}_{k+1}\mathbf{u}_{k+1}$. Then, using also (14), we find that the downward mode amplitude at boundary z_k is

$$\begin{aligned}\mathbf{d}_k &= \mathsf{P}^{\mathrm{d}}_k\mathbf{d}'_{k+1} = \mathsf{P}^{\mathrm{d}}_k\left(\mathsf{T}^{\mathrm{d}}_{k,du}\mathbf{u}_{k+1} + \mathsf{T}^{\mathrm{d}}_{k,dd}\mathbf{d}_{k+1}\right)\\ &= \mathsf{P}^{\mathrm{d}}_k\left(\mathsf{T}^{\mathrm{d}}_{k,du} + \mathsf{T}^{\mathrm{d}}_{k,dd}\mathsf{R}^{\mathrm{u}}_{k+1}\right)\mathbf{u}_{k+1}\end{aligned} \tag{24}$$

where we used equation (18) written in a block-matrix form, so that $\mathsf{T}^{\mathrm{d}}_{k,du}$ and $\mathsf{T}^{\mathrm{d}}_{k,dd}$ are 2×2 submatrices of $\mathsf{T}^{\mathrm{d}}_k$. On the other hand, $\mathbf{d}_k = \mathsf{R}^{\mathrm{u}}_k\mathbf{u}_k$ and

$$\begin{aligned}\mathbf{u}_k &= \left(\mathsf{P}^{\mathrm{u}}_k\right)^{-1}\mathbf{u}'_{k+1} = \left(\mathsf{P}^{\mathrm{u}}_k\right)^{-1}\left(\mathsf{T}^{\mathrm{d}}_{k,uu}\mathbf{u}_{k+1} + \mathsf{T}^{\mathrm{d}}_{k,ud}\mathbf{d}_{k+1}\right)\\ &= \left(\mathsf{P}^{\mathrm{u}}_k\right)^{-1}\left(\mathsf{T}^{\mathrm{d}}_{k,uu} + \mathsf{T}^{\mathrm{d}}_{k,ud}\mathsf{R}^{\mathrm{u}}_{k+1}\right)\mathbf{u}_{k+1}\end{aligned} \tag{25}$$

From these two results, since they should hold for arbitrary $\mathbf{u}_{k+1}$, we obtain the recursive relation for $\mathsf{R}^{\mathrm{u}}_k$, the reflection coefficient from above:

$$\mathsf{R}^{\mathrm{u}}_k = \mathsf{P}^{\mathrm{d}}_k\left(\mathsf{T}^{\mathrm{d}}_{k,du} + \mathsf{T}^{\mathrm{d}}_{k,dd}\mathsf{R}^{\mathrm{u}}_{k+1}\right)\left(\mathsf{T}^{\mathrm{d}}_{k,uu} + \mathsf{T}^{\mathrm{d}}_{k,ud}\mathsf{R}^{\mathrm{u}}_{k+1}\right)^{-1}\mathsf{P}^{\mathrm{u}}_k \tag{26}$$

Analogously, we obtain a recursive relation for the reflection coefficient from below:

$$\mathsf{R}^{\mathrm{d}}_{k+1} = \left(\mathsf{T}^{\mathrm{u}}_{k,uu}\mathsf{P}^{\mathrm{u}}_k\mathsf{R}^{\mathrm{d}}_k\mathsf{P}^{\mathrm{d}}_k + \mathsf{T}^{\mathrm{u}}_{k,ud}\right)\left(\mathsf{T}^{\mathrm{u}}_{k,du}\mathsf{P}^{\mathrm{u}}_k\mathsf{R}^{\mathrm{d}}_k\mathsf{P}^{\mathrm{d}}_k + \mathsf{T}^{\mathrm{u}}_{k,dd}\right)^{-1} \tag{27}$$

Both of these equations are stable when n_z have large imaginary parts because the matrices P^{u}, P^{d} are bounded. The recursive formulas (26) and (27) must use initial values for $\mathsf{R}^{\mathrm{u}}_M$ and $\mathsf{R}^{\mathrm{d}}_1$. We assume that the upper boundary is free, so we have $\mathsf{R}^{\mathrm{u}}_M = 0$. For a conducting Earth, we have $\mathbf{E}_\perp = 0$ at $z = z_1$. Substituting $\mathbf{E}_\perp = 0$ and $\mathbf{u}_1 = \mathsf{R}^{\mathrm{d}}_1\mathbf{d}_1$ into (10), we find that $\mathsf{R}^{\mathrm{d}}_1 = -(\mathsf{F}_{1,Eu})^{-1}\mathsf{F}_{1,Ed}$, where, e.g., $\mathsf{F}_{k,Eu}$ is a 2×2 submatrix of F_k with rows corresponding to $\mathbf{E}_\perp$ and columns corresponding to $\mathbf{u}$. In an isotropic medium, using (9) we obtain $\mathsf{R}^{\mathrm{d}}_1 = -\mathsf{I}$.

2.3. Calculation of Mode Amplitudes

[12] Now, let us derive recursive relations for $\mathbf{u}$ above the sources and $\mathbf{d}$ below the sources (the mode amplitudes for the other direction are obtained using the reflection coefficients, see equations (22)–(23)). Let us express $\mathbf{u}_{k+1}$ in terms of $\mathbf{u}_k$, using (19) and (13)–(14):

$$\begin{aligned}\mathbf{u}_{k+1} &= \mathsf{T}^{\mathrm{u}}_{k,uu}\mathbf{u}'_{k+1} + \mathsf{T}^{\mathrm{u}}_{k,ud}\mathbf{d}'_{k+1}\\ &= \mathsf{T}^{\mathrm{u}}_{k,uu}\mathsf{P}^{\mathrm{u}}_k\mathbf{u}_k + \mathsf{T}^{\mathrm{u}}_{k,ud}\left(\mathsf{P}^{\mathrm{d}}_k\right)^{-1}\mathbf{d}_k\\ &= \left(\mathsf{T}^{\mathrm{u}}_{k,uu}\mathsf{P}^{\mathrm{u}}_k + \mathsf{T}^{\mathrm{u}}_{k,ud}\left(\mathsf{P}^{\mathrm{d}}_k\right)^{-1}\mathsf{R}^{\mathrm{u}}_k\right)\mathbf{u}_k\end{aligned} \tag{28}$$

Thus, we have the recursive relation sought

$$\mathbf{u}_{k+1} = U_k\mathbf{u}_k \tag{29}$$

where

$$U_k = \mathsf{T}^{\mathrm{u}}_{k,uu}\mathsf{P}^{\mathrm{u}}_k + \mathsf{T}^{\mathrm{u}}_{k,ud}\left(\mathsf{P}^{\mathrm{d}}_k\right)^{-1}\mathsf{R}^{\mathrm{u}}_k \tag{30}$$

There is no potential instability in (30) from $(\mathsf{P}^{\mathrm{d}}_k)^{-1}$ because it cancels with $\mathsf{P}^{\mathrm{d}}_k$ in the expression for the reflection coefficient (26). Analogously, we find that below the sources

$$\mathbf{d}_k = \mathsf{D}_k\mathbf{d}_{k+1} \tag{31}$$

where

$$\mathsf{D}_k = \mathsf{P}^{\mathrm{d}}_k\left(\mathsf{T}^{\mathrm{d}}_{k,du}\mathsf{R}^{\mathrm{d}}_{k+1} + \mathsf{T}^{\mathrm{d}}_{k,dd}\right) \tag{32}$$

which is also stable.

2.4. Dealing With the Sources

[13] Assume that horizontal currents have harmonic dependence on time and perpendicular coordinates, i.e., $\sim e^{ik_0(\mathbf{n}_\perp\cdot\mathbf{r}_\perp)-i\omega t}$ and flow only in the plane $z = z_s + 0$, just above the boundary between layers Ω_{s-1} and Ω_s, so that they are still inside Ω_s:

$$\mathbf{J}(\mathbf{r}, t) = \mathbf{I}_\perp\delta(z - z_s)e^{ik_0(\mathbf{n}_\perp\cdot\mathbf{r}_\perp)-i\omega t} \tag{33}$$

Our task is to find the wave amplitudes $\mathbf{u}(z)$ and $\mathbf{d}(z)$ inside layer Ω_s just above ($\mathbf{u}^+_s$, $\mathbf{d}^+_s$) and just below ($\mathbf{u}^-_s$, $\mathbf{d}^-_s$) the source plane.

[14] The fields satisfy boundary conditions

$$\Delta\mathbf{E}_\perp \equiv \mathbf{E}^+_s - \mathbf{E}^-_s = 0 \tag{34}$$

$$\Delta\mathbf{H}_\perp \equiv \mathbf{H}^+_s - \mathbf{H}^-_s = (Z_0\mathbf{I}_\perp \times \hat{z}) \tag{35}$$

These conditions are obtained by integration of one of the Maxwell's equations across the boundary and are valid in an arbitrary nonmagnetic medium (i.e., the permeability $\mu \equiv 1$). The changes $\Delta\mathbf{E}_\perp$, $\Delta\mathbf{H}_\perp$ in the presence of vertical currents are derived in Appendix A. For the application considered in section 3 below, however, only equations (34)–(35) are sufficient, because the vertical currents are negligible.

[15] The change $\Delta\mathbf{u}$ and $\Delta\mathbf{d}$ at the plane of the source is obtained using (10):

$$\begin{pmatrix}\Delta\mathbf{u}\\ \Delta\mathbf{d}\end{pmatrix} = \mathsf{F}^{-1}_s\begin{pmatrix}\Delta\mathbf{E}_\perp\\ \Delta\mathbf{H}_\perp\end{pmatrix} \tag{36}$$

Since there are no sources other than at z_s, we can use reflection coefficients (22) and (23) to relate $\mathbf{u}^\pm_s$ and $\mathbf{d}^\pm_s$:

$$\mathbf{d}^+_s = \mathsf{R}^{\mathrm{u}}_s\mathbf{u}^+_s \tag{37}$$

$$\mathbf{u}^-_s = \mathsf{R}^{\mathrm{d}}_s\mathbf{d}^-_s \tag{38}$$

Substituting

$$\mathbf{u}_s^- = \mathbf{u}_s^+ - \Delta\mathbf{u} \tag{39}$$

$$\mathbf{d}_s^- = \mathbf{d}_s^+ - \Delta\mathbf{d} \tag{40}$$

we find the solution

$$\mathbf{u}_s^+ = \left(\mathsf{I} - \mathsf{R}_s^{\mathrm{d}}\mathsf{R}_s^{\mathrm{u}}\right)^{-1}\left(\Delta\mathbf{u} - \mathsf{R}_s^{\mathrm{d}}\Delta\mathbf{d}\right) \tag{41}$$

$$\mathbf{d}_s^+ = \mathsf{R}_s^{\mathrm{u}}\mathbf{u}_s^+ \tag{42}$$

Now we can find all $\mathbf{u}_k$ and $\mathbf{d}_k$ at all altitudes, using (29) and (31), e.g., $\mathbf{u}_{s+1} = U_s\mathbf{u}_s^+$, $\mathbf{d}_{s-1} = \mathsf{D}_{s-1}\mathbf{d}_s^-$ etc. Then, the reflected waves are obtained using the reflection coefficients, i.e., $\mathbf{d}_{s+1} = \mathsf{R}_{s+1}^{\mathrm{u}}\mathbf{u}_{s+1}$, $\mathbf{u}_{s-1} = \mathsf{R}_{s-1}^{\mathrm{d}}\mathbf{d}_{s-1}$, etc., thus constructing the complete full-wave solution in all layers. Note that (41) does not give a valid answer if $\det(\mathsf{I} - \mathsf{R}_s^{\mathrm{d}}\mathsf{R}_s^{\mathrm{u}}) = 0$, which is the resonance condition. However, since there are always some losses in the medium, the resonance condition cannot be satisfied for real $\mathbf{n}_\perp$.

[16] If the sources occupy more than one layer, we can find the total field by summing fields created by each layer. To accelerate calculations, we can introduce auxiliary variables $\mathbf{u}^{\mathrm{up}}$ (the upward modes only from the sources below observation altitude) and $\mathbf{d}^{\mathrm{down}}$ (the downward modes only from the sources above the observation altitude). These can be calculated recursively:

$$\mathbf{u}_{k+1}^{\mathrm{up}} = \mathbf{u}_{k+1}^+ + U_k\mathbf{u}_k^{\mathrm{up}}$$
$$\mathbf{d}_k^{\mathrm{down}} = \mathsf{D}_k\left(\mathbf{d}_{k+1}^{\mathrm{down}} + \mathbf{d}_{k+1}^-\right)$$

The full wave solution is obtained by adding the reflected waves, i.e., the upward modes from sources above the observation altitude and downward modes from sources below the observation altitude:

$$\mathbf{u}_k = \mathbf{u}_k^{\mathrm{up}} + \mathsf{R}_k^{\mathrm{d}}\mathbf{d}_k^{\mathrm{down}}$$
$$\mathbf{d}_k = \mathbf{d}_k^{\mathrm{down}} + \mathsf{R}_k^{\mathrm{u}}\mathbf{u}_k^{\mathrm{up}}$$

[17] If the source region has an arbitrary shape, we use the horizontal Fourier decomposition of the sources, at each altitude:

$$\mathbf{J}_\perp(\mathbf{n}_\perp, z) = \iint \mathbf{J}_\perp(\mathbf{r}_\perp, z)e^{-ik_0(\mathbf{n}_\perp\cdot\mathbf{r}_\perp)}d^2\mathbf{r}_\perp \tag{43}$$

We use the algorithm described above to calculate fields $\mathbf{E}(\mathbf{n}_\perp, z)$ and $\mathbf{H}(\mathbf{n}_\perp, z)$ which are radiated by $\mathbf{J}_\perp(\mathbf{n}_\perp, z)$. Then, we use the inverse transform to calculate the total fields:

$$\mathbf{E}(\mathbf{r}_\perp, z) = \iint \mathbf{E}(\mathbf{n}_\perp, z)e^{ik_0(\mathbf{n}_\perp\cdot\mathbf{r}_\perp)}\frac{k_0^2 d^2\mathbf{n}_\perp}{(2\pi)^2}$$
$$\mathbf{H}(\mathbf{r}_\perp, z) = \iint \mathbf{H}(\mathbf{n}_\perp, z)e^{ik_0(\mathbf{n}_\perp\cdot\mathbf{r}_\perp)}\frac{k_0^2 d^2\mathbf{n}_\perp}{(2\pi)^2}$$

Using a discrete Fourier decomposition forces us to have periodic boundary conditions at the side boundaries. We should choose these boundaries far enough so that the waves are attenuated in the horizontal direction to the degree that the sources in the next horizontal "period" do not change the results in the computational domain. The method can be applied both in 2-D and in 3-D. In the 2-D case, the Fourier decomposition is only over one of the horizontal components of $\mathbf{n}_\perp$.

3. Application to the Problem of a Modulated Electrojet in an HF-Heated Ionosphere

[18] The magnetized plasma dielectric tensor for geomagnetic $\mathbf{B}_0 \| \hat{z}$ is [*Stix*, 1992]

$$\hat{\varepsilon}_z = \begin{pmatrix} S & -iD & 0 \\ iD & S & 0 \\ 0 & 0 & P \end{pmatrix} \tag{44}$$

For an electron plasma with collisions we use $S = (R + L)/2$, $D = (R - L)/2$, with R, L, and P given by

$$R = 1 - \frac{\omega_p^2}{\omega(\omega + i\nu - \omega_H)}$$
$$L = 1 - \frac{\omega_p^2}{\omega(\omega + i\nu + \omega_H)}$$
$$P = 1 - \frac{\omega_p^2}{\omega(\omega + i\nu)}$$

where ω_p is the plasma frequency, ω_H is the electron gyrofrequency, and ν is the electron collision frequency. In a general case of an arbitrary direction of $\mathbf{B}_0$, the dielectric tensor $\hat{\varepsilon}$ is obtained by rotating $\hat{\varepsilon}_z$ from an appropriately chosen coordinate system in which $\hat{z'} \| \mathbf{B}_0$ to a system with vertical $\hat{z}$.

[19] As an example, we calculate the fields created by electrojet currents modulated at frequency of 1875 Hz by the HAARP HF heating facility (as of April 2003). The change in the electrojet currents is calculated by *Payne et al.* [2007], for heating of the ionosphere by a sinusoidally modulated fully focused HF beam at 3.2 MHz and effective radiated power (ERP) of ~24 MW. The x-axis is chosen in the eastward direction, and y-axis in the northward direction. The modulated currents are horizontal, and occupy a volume which has a shape of a horizontal pancake, with a slice shown in Figure 1a and the profile at the central vertical axis shown in Figure 1b. The altitude-dependent geomagnetic field is calculated using the IGRF model (http://modelweb.gsfc.nasa.gov/models/igrf.html) for the HAARP site and has components $\mathbf{B}_0 \simeq \{6 \times 10^{-6}, 1.3 \times 10^{-5}, -5.3 \times 10^{-5}\}$ T at the altitude of the D-region currents. The electron density and collision frequency profiles are assumed to be the same as in [*Payne et al.*, 2007], with electron density profile extended to higher altitudes using the IRI model (http://modelweb.gsfc.nasa.gov/models/iri.html). A vertical slice of two components of calculated fields is shown in Figure 2 and is discussed below in regard to satellite and ground-based observations.

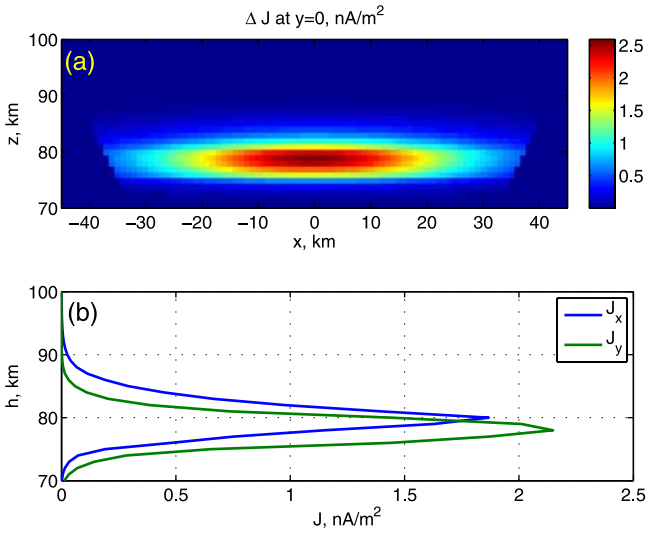

Figure 1. (a) Absolute value of the amplitude of modulated current density at $y = 0$. The vertical currents are negligible, and the horizontal currents are due to Pedersen and Hall mechanisms. (b) The components of the current density at $x = 0$, $y = 0$. The electrojet ambient field is $E_0 = \hat{x}(-25\ \text{mV})$, so J_x corresponds to Pedersen and J_y to Hall current.

3.1. Upward Propagating Fields and Comparison With Satellite Observations

[20] The horizontal refractive index $\mathbf{n}_\perp$ of the wave propagating through the stratified medium is conserved due to Snell's law. Owing to this fact, the radiated whistler waves at the satellite altitude can contain only components with the same $\mathbf{n}_\perp$ as were present in the horizontal Fourier transform $\mathbf{J}_\perp(\mathbf{n}_\perp, z)$ of the source $\mathbf{J}_\perp(\mathbf{r}_\perp, z)$ (see equation (43)). Because of the large horizontal size of the region occupied by the radiating currents $L \simeq 50$ km (Figure 1a), the horizontal components of the refractive index $n_\perp = k_\perp/k_0 \simeq (k_0 L)^{-1} \lesssim 1$ of the components present in the radiated waves are not very large, especially compared to the refractive index of the whistler mode at the satellite altitudes (~700 km), which is of the order of $n \sim 60$. This fact is illustrated in Figure 3, in which we plot both the refractive index surface and $|\mathbf{J}_\perp(\mathbf{n}_\perp, z)|$. The group velocities of the upward radiated whistler-mode components are therefore almost parallel, and these waves form a narrow collimated beam which does not have much lateral spread. The collimated beam can be seen in Figures 2a and 4.

[21] The vertical energy flux (Poynting vector) $S_z = (2Z_0)^{-1}\text{Re}[(\mathbf{E}^*_\perp)_M \times (\mathbf{H}_\perp)_M]_z$ calculated at the boundary of the last layer Ω_M which is at the satellite altitude of $h = z_M = 700$ km is shown in Figure 4. The maximum fields are $E_{\max} \simeq 150\ \mu\text{V m}^{-1}$ and $B_{\max} \simeq 30$ pT and occupy a spot of the size similar to the size of the heated region, ~50 km in diameter. The fields are an order of magnitude lower in a larger spot of ~100–200 km diameter and decrease very fast at larger distances from the center. The calculated fields are larger than $E_{\max} \simeq 2\ \mu\text{V m}^{-1}$ and $B_{\max} \simeq 0.5$ pT measured by the Akebono satellite above the Tromsø heating facility in Norway [*Kimura et al.*, 1994], which is probably due to (1) a lower heating power than HAARP; and (2) the fact that the satellite was outside the narrow region where the maximum field is achieved.

[22] Recent observations under similar conditions (HF frequency of 3.25 MHz and modulation at 2 kHz) by the DEMETER satellite indicate values as high as $E_{\max} \simeq 350\ \mu\text{V m}^{-1}$ and $B_{\max} \simeq 20$ pT in a narrow collimated beam corresponding to the size (~10 km) of the radiating currents region (D. Piddyachiy et al., DEMETER observations of ELF signal generated by the HAARP HF heater, submitted to *Geophysical Research Letters*, 2008). However, these measurements were made for the upgraded HAARP facility, with a higher effective radiated power (ERP) of ~350 MW and a narrower beam (which explains a smaller radiating region). The total energy emitted upward is calculated by integrating the vertical Poynting flux and is equal to ≃3 W for the considered example, which is inside the range 0.32–4 W previously estimated from observations by DEMETER (before the upgrade) [*Platino et al.*, 2006].

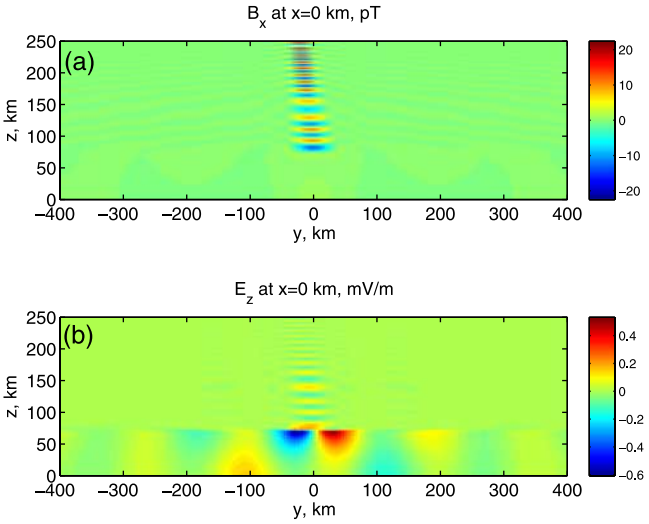

Figure 2. Fields in the $x = 0$ plane: (a) B_x; (b) E_z, showing (top) the formation of the whistler collimated beam and (bottom) the propagation in the Earth-ionosphere waveguide.

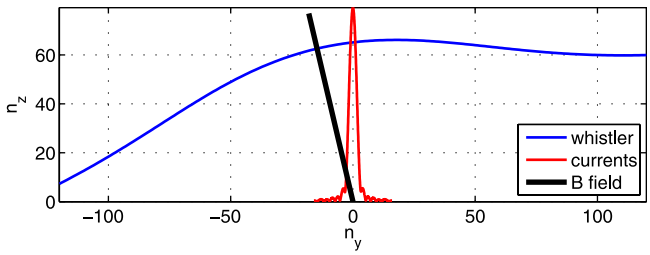

Figure 3. Blue line shows a slice of the refractive index surface at $n_x = 0$ of the whistler mode, calculated for $f = 1875$ Hz at the satellite altitude of $h = 700$ km. Black line shows the direction of the geomagnetic field. Red line shows the absolute value of the horizontal Fourier transform of the currents $|\mathbf{J}_\perp(\mathbf{n}_\perp, z)|$ given in equation (43) and calculated at $z = 77$ km (where the currents are maximized) and $n_x = 0$. The vertical scale of the red line is arbitrary.

3.2. Comparison With Ground-Based Observations

[23] The calculated ground-based horizontal magnetic field $\mathbf{B}_\perp = (\mathbf{H}_\perp)_1/c$ and vertical electric field $(E_z)_1$ are shown in Figure 5. The magnetic field $\mathbf{B}_\perp \simeq 1-2$ pT is similar to the field measured at VLF sites in immediate vicinity of HAARP heating facility [*Payne et al.*, 2007]. The fields show the concentric structure of ELF waves propagating in the Earth-ionosphere waveguide. The ELF mode structure at all altitudes is shown in Figure 2b. The total emission power into the Earth-ionosphere waveguide can be calculated by integrating the horizontal Poynting flux through the boundary of a box enclosing the source currents, and is estimated to be $\simeq$1 W (at the distance of 50 km from the central axis), which is slightly below the range 2.71–4.22 W obtained by *Platino et al.* [2006].

4. Discussion

[24] The proposed method uses the idea due to *Nygrén* [1982] for recursive calculation of both the reflection coefficients and the wave amplitudes, the direction of recursion being important for the stability against "swamping." For example, for upward propagating waves the recursion is $\mathsf{R}^{\mathrm{u}}_{k+1} \rightarrow \mathsf{R}^{\mathrm{u}}_{k}$ and $\mathbf{u}_k \rightarrow \mathbf{u}_{k+1}$. This first relation can be understood as insertion of an additional slab of a refracting medium in the path of an upward propagating wave, which modifies the old reflection coefficient. The second relation is just following the direction of the wave propagation. Thus, the direction of the recursive calculation has a simple causal physical meaning, which probably explains the stability of the method against "swamping."

[25] The calculations in the heating example are performed assuming a stratified medium, i.e., we neglect the change of conductivity in a small region caused by heating, and consider the modulated electrojet currents as an external source radiating in an unmodified ionosphere. The maximum change in conductivity occurs at 80 km and is equal to

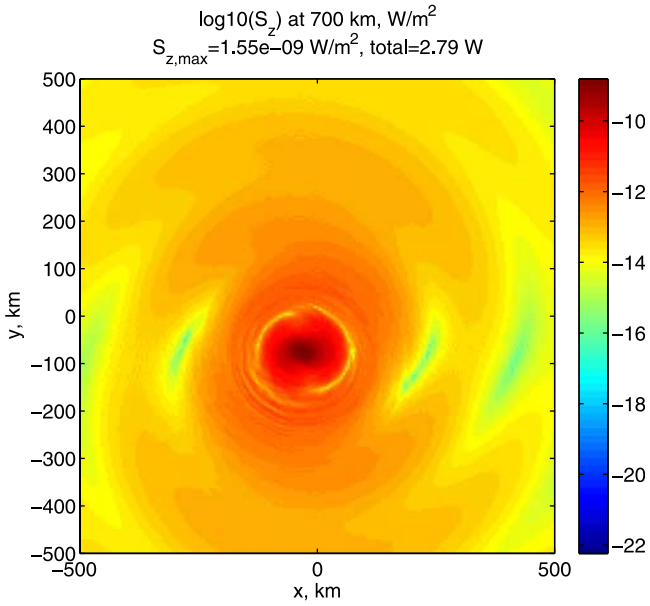

Figure 4. The calculated vertical Poynting vector at h = 700 km.

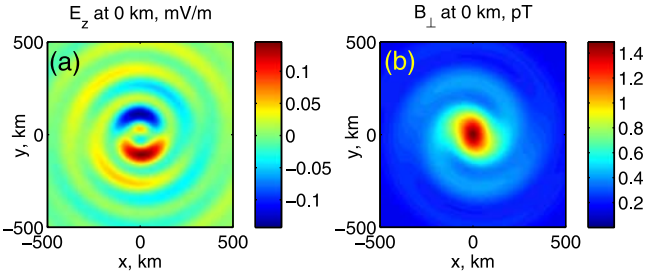

Figure 5. The calculated fields at h = 0 km: (a) E_z; (b) $B_\perp$.

$\sim$80 nS m^{-1} (for both Pedersen and Hall components) [*Payne et al.*, 2007]. This equals to relative changes of 22.5% for Pedersen and 3.5% for Hall components of the background conductivity. Since we neglect the effect of this change on the propagation of the electromagnetic waves in our calculations, we expect relative errors of the same order in the calculated fields.

5. Conclusions

[26] We have developed a stable method for calculation of waves in a stratified medium which are created by an arbitrary combination of harmonically varying sources, with arbitrary electromagnetic properties of the medium (i.e., permittivity tensor $\hat{\varepsilon}$). Currently, the only drawback of the application of this method to the generation of electromagnetic waves in the Earth-ionosphere waveguide and ionosphere by ionospheric heaters is that the curvature of the Earth is not taken into account. However, the method presented herein can be modified by including small corrections for the curvature.

Appendix A: Boundary Conditions When Crossing a Double Layer

[27] Consider the field generated in vacuum by a current and charge density given by

$$\mathbf{J}(\mathbf{r},t) = \hat{z} I \delta(z) e^{ik_x x - i\omega t} \tag{A1}$$

$$\rho(\mathbf{r},t) = \frac{I\delta'(z)}{i\omega} e^{ik_x x - i\omega t} \tag{A2}$$

where ρ has been found from $\mathbf{J}$ using the continuity equation $\nabla \cdot \mathbf{J} + \dot{\rho} = 0$. Potentials conforming with the Lorenz gauge condition $\nabla \cdot \mathbf{A} + \varepsilon_0\mu_0\dot{\phi} = 0$ satisfy equations

$$\nabla^2 \mathbf{A} - \varepsilon_0\mu_0 \ddot{\mathbf{A}} = -\mu_0 \mathbf{J} \tag{A3}$$

$$\nabla^2 \phi - \varepsilon_0\mu_0 \ddot{\phi} = -\rho/\varepsilon_0 \tag{A4}$$

For the sources given by (A1)–(A2), we look for a solution in the form $\mathbf{A}(\mathbf{r}, t) = \hat{z} A_z(z) e^{ik_x x - i\omega t}$ and $\phi(\mathbf{r}, t) = \phi(z) e^{ik_x x - i\omega t}$. Equation (A4) becomes:

$$k_z^2 \phi(z) + \partial_{zz}\phi(z) = -\frac{I\delta'(z)}{i\omega\varepsilon_0} \tag{A5}$$

where $k_z = \sqrt{k_0^2 - k_x^2}$ and $k_0 = \omega/c$. Solving for $\phi(z)$ and obtaining $A_z(z)$ from the gauge condition, we find

$$\phi(\mathbf{r}, t) = -\frac{I\,\mathrm{sign}(z)}{2i\omega\varepsilon_0} e^{ik_z|z| + ik_x x - i\omega t} \tag{A6}$$

$$\mathbf{A}(\mathbf{r}, t) = -\hat{z}\frac{I\mu_0}{2ik_z} e^{ik_z|z| + ik_x x - i\omega t} \tag{A7}$$

The fields are found from $\mathbf{E}(\mathbf{r}, t) = -\nabla\phi - \dot{\mathbf{A}}$, $\mathbf{H}(\mathbf{r}, t) = c\nabla \times \mathbf{A}$ (we use $\mathbf{H} \equiv Z_0\mathbf{H}_{\mathrm{SI}}$, as in the main text of this paper). Substituting expressions for ϕ and $\mathbf{A}$, we find

$$\mathbf{E}(\mathbf{r}, t) = \frac{Z_0 I}{2}\left(\hat{x}n_x \mathrm{sign}(z) - \hat{z}\frac{n_x^2}{n_z}\right) e^{ik_z|z| + ik_x x - i\omega t} + \hat{z}\frac{Z_0 I}{ik_0}\delta(z) e^{ik_x x - i\omega t} \tag{A8}$$

$$\mathbf{H}(\mathbf{r}, t) = \hat{y}\frac{Z_0 I}{2}\frac{n_x}{n_z} e^{ik_z|z| + ik_x x - i\omega t} \tag{A9}$$

where $n_x = k_x/k_0$, $n_z = k_z/k_0$ and $Z_0 = \sqrt{\mu_0/\varepsilon_0}$. The change in the perpendicular component of $\mathbf{E}$ is

$$\Delta\mathbf{E}_\perp = \mathbf{E}_\perp|_{z=+0} - \mathbf{E}_\perp|_{z=-0} = Z_0 I\mathbf{n}_\perp \tag{A10}$$

where $\mathbf{n}_\perp = \hat{x}n_x$, and we omitted the factor $e^{ik_x x - i\omega t}$. We also see that $\Delta\mathbf{H}_\perp = 0$. In the configuration space, for $\mathbf{J}(\mathbf{r}, t) = \hat{z}I(\mathbf{r}_\perp)\delta(z)e^{-i\omega t}$, the last relation becomes

$$\Delta\mathbf{E}_\perp(\mathbf{r}_\perp) = \frac{Z_0}{ik_0}\nabla_\perp I(\mathbf{r}_\perp) e^{-i\omega t} \tag{A11}$$

For an arbitrary uniform nonmagnetic medium with the dielectric permittivity tensor $\hat{\varepsilon}$ with components ε_{ij}, $i, j = x, y, z$, the derivation of the boundary conditions is done by integrating the Maxwell's equations through the boundary layer [*Lehtinen and Inan*, 2007]:

$$\Delta\mathbf{E}_\perp = \frac{Z_0 I\mathbf{n}_\perp}{\varepsilon_{zz}} \tag{A12}$$

$$\Delta\mathbf{H}_\perp = \left(Z_0\mathbf{I}_{\mathrm{pol}} \times \hat{z}\right) \tag{A13}$$

where the horizontal polarization current $\mathbf{I}_{\mathrm{pol}}$ is induced due to off-diagonal components in the dielectric permittivity tensor and is given by $\mathbf{I}_{\mathrm{pol}} = -I(\varepsilon_{xz}\hat{x} + \varepsilon_{yz}\hat{y})/\varepsilon_{zz}$.

[28] **Acknowledgments.** This work was supported by the High-Frequency Active Auroral Research Program (HAARP), the Air Force Research Laboratory (AFRL), the Defense Advanced Research Program Agency (DARPA), and the Office of Naval Research (ONR) via ONR grant N00014-05-1-0854 to Stanford University.

[29] Amitava Bhattacharjee thanks Masao Ozaki and another reviewer for their assistance in evaluating this paper.

References

Abramowitz, M., and I. A. Stegun (Eds.) (1970), *Handbook of Mathematical Functions With Formulas, Graphs and Mathematical Tables*, 9th ed., Dover, New York.

Booker, H. G. (1938), Propagation of wave-packets incident obliquely upon a stratified doubly refracting ionosphere, *Phil. Trans. R. Soc. London, Ser. A*, *237*(781), 411–451.

Bossy, L. (1979), Wave propagation in stratified anisotropic media, *J. Geophys.*, *46*, 1–14.

Budden, K. G. (1985), *The Propagation of Radio Waves: The Theory of Radio Waves of Low Power in the Ionosphere and Magnetosphere*, Cambridge Univ. Press, Cambridge, U.K.

Kimura, I., P. Stubbe, M. T. Rietveld, R. Barr, K. Ishida, Y. Kasahara, S. Yagitani, and I. Nagano (1994), Collaborative experiments by Akebono satellite, Tromsø ionospheric heater, and European incoherent scatter radar, *Radio Sci.*, *29*(1), 32–37, doi:10.1029/93RS01727.

Lehtinen, N. G., and U. S. Inan (2007), Emission of ELF/VLF waves by a modulated electrojet upwards into the ionosphere and indo the earth-ionosphere waveguide, *Eos Trans. AGU*, *88*(52), Fall Meet. Suppl., Abstract SA11A-0297.

Nagano, I., K. Miyamura, S. Yagitani, I. Kimura, T. Okada, K. Hashimoto, and A. Y. Wong (1994), Full wave calculation method of VLF wave radiated from a dipole antenna in the ionosphere– analysis of joint experiment by HIPAS and Akebono satellite, *Electr. Commun. Jpn. Commun.*, *77*(11), 59–71, doi:10.1002/ecja.4410771106.

Nygrén, T. (1981), A simple method for obtaining reflection and transmission coefficients and fields for an electromagnetic wave in a horizontally stratified ionosphere, *Planet Space Sci.*, *29*(5), 521–528, doi:10.1016/0032-0633(81)90066-0.

Nygrén, T. (1982), A method of full wave analysis with improved stability, *Planet. Space Sci.*, *30*(4), 427–430, doi:10.1016/0032-0633(82)90048-4.

Payne, J. A., U. S. Inan, F. R. Foust, T. W. Chevalier, and T. F. Bell (2007), HF modulated ionospheric currents, *Geophys. Res. Lett.*, *34*, L23101, doi:10.1029/2007GL031724.

Pitteway, M. L. V. (1965), The numerical calculation of wave-fields, reflexion coefficients and polarizations for long radio waves in the lower ionosphere I, *Phil. Trans. R. Soc. London, Ser. A*, *257*(1079), 219–241.

Platino, M., U. S. Inan, T. F. Bell, M. Parrot, and E. J. Kennedy (2006), DEMETER observations of ELF waves injected with the HAARP HF transmitter, *Geophys. Res. Lett.*, *33*, L16101, doi:10.1029/2006GL026462.

Stix, T. (1992), *Waves in Plasmas*, Springer, New York.

Wait, J. R. (1970), *Electromagnetic Waves in Stratified Media*, 2nd ed., Pergamon, New York.

Yagitani, S., I. Nagano, K. Miyamura, and I. Kimura (1994), Full wave calculation of ELF/VLF propagation from a dipole source located in the lower ionosphere, *Radio Sci.*, *29*(1), 39–54, doi:10.1029/93RS01728.

U. S. Inan and N. G. Lehtinen, STARLab, Electrical Engineering Department, Stanford University, Stanford, CA 94040, USA. (nleht@stanford.edu)